Published in final edited form as:
J Neurosci Res. 2007 April ; 85(5): 1126–1137. doi:10.1002/jnr.21210.

Adenosine Inhibits Voltage-Dependent Ca^{2+} Influx in Cone Photoreceptor Terminals of the Tiger Salamander Retina

Salvatore L. Stella Jr.[1,2,3,⋆], **Wanda D. Hu**[1], **Alejandro Vila**[1,2,3], and **Nicholas C. Brecha**[1,2,3]

[1]Department of Neurobiology, David Geffen School of Medicine, University of California, Los Angeles, California

[2]Department of Medicine David Geffen School of Medicine, University of California, Los Angeles, California

[3]Jules Stein Eye Institute, David Geffen School of Medicine, University of California, Los Angeles, California

[4]Veterans Affairs Greater Los Angeles Healthcare System, Los Angeles, California

Abstract

Endogenous adenosine has already been shown to inhibit transmitter release from the rod synapse by suppressing Ca^{2+} influx through voltage-gated Ca^{2+} channels. However, it is not clear how adenosine modulates the cone synapse. Cone photoreceptors, like rod photoreceptors, also possess L-type Ca^{2+} channels that regulate the release of L-glutamate. To assess the impact of adenosine on Ca^{2+} influx though voltage-gated Ca^{2+} channels in cone terminals, whole-cell perforated-patch clamp recording and Ca^{2+} imaging with fluo-4 were used on isolated cones and salamander retinal slices. Synaptic markers (VAMP and piccolo) and activity-dependent dye labeling revealed that tiger salamander cone terminals contain a broad, vesicle-filled cytoplasmic extension at the base of the somatic compartment, which is unlike rod terminals that contain one or more thin axons, each terminating in a large bulbous synaptic terminal. The spatiotemporal Ca^{2+} responses of the cone terminals do not differ significantly from the Ca^{2+} responses of the soma or inner segment like that observed in rods. Whole-cell recording of cone I_{Ca} and Ca^{2+} imaging of synaptic terminals in cones demonstrate that adenosine inhibited both I_{Ca} and the depolarization-evoked Ca^{2+} increase in cone terminals in a dose-dependent manner from 1 to 50 μM, with an EC_{50} of 15.6 μM. These results indicate that, as in rods, adenosine's ability to suppress voltage-dependent Ca^{2+} channels at the cone synapse will limit the amount of L-glutamate released. Therefore, adenosine has an inhibitory effect on L-glutamate release at the first synapse, which likely favors elevated adenosine levels in the dark or during dark-adapted conditions.

Keywords

FM 4-64; Synaptored-C2; fluo-4; VAMP; piccolo

In the retina, adenosine has been shown to be under tight regulation by light and dark conditions (Ribelaya and Mangel, 2005), and it is the changing conditions of illumination that influence adenosine levels (Blazanski and Perez, 1991; Paes de Carvalho, 2002; Sun et al., 2002; Stella et al., 2003; Ribelaya and Mangel, 2005), making adenosine concentrations higher in the dark and lower in the light. Adenosine can also inhibit Ca^{2+} channels and

⋆Correspondence to: Salvatore L. Stella, Jr., Neurobiology Department, David Geffen School of Medicine, University of California Los Angeles, 10833 Le Conte Ave., Box 951763, CHS 73-323, Los Angeles, CA 90095-1763. sstella@mednet.ucla.edu.

transmitter release from rods (Stella et al., 2002, 2003), suggesting that adenosine levels might play a pivotal role in the regulation of the first synapse in visual processing. Consistent with this idea, the retina, like the brain, expresses the receptors (Braas et al., 1987; Blazynski, 1990; Rey and Burnside, 1999; Stella et al., 2002, 2003), enzymes (Roth et al., 1997), and adenosine transporters (Blazynski et al., 1989; Studholme and Yazulla, 1997; Ribelaya and Mangel, 2005) involved in the regulation of adenosine. However, the physiological role of adenosine in the outer retina and its action at the cone synapse are incompletely understood.

The presence of adenosine and adenosine receptors in the outer retina and particularly photoreceptors has been demonstrated by autoradiography, in situ hybridization, and pharmacological studies (Blazynski, 1990; Kvanta et al., 1997; Rey and Burnside, 1999; Stella et al., 2002, 2003), suggesting that both cones and rods contain adenosine receptors. In rods, adenosine has been shown to inhibit L-type Ca^{2+} channels via A_2-like receptors through a cAMP-dependent protein kinase A (PKA)-mediated pathway, thereby suppressing transmitter release from rods onto second-order neurons (Stella et al., 2002, 2003). In addition, the A_{2A} antagonist ZM-214385 alone can enhance postsynaptic light responses from second-order neurons, suggesting that endogenous adenosine is present in the outer retina, and adenosine has a strong tonic inhibitory role at the rod synapse (Stella et al., 2002, 2003). In addition, Barnes and Hille (1989) showed that adenosine can inhibit the Ca^{2+}-activated chloride current in cones, suggesting the possibility that Ca^{2+} influx through voltage-gated Ca^{2+} channels is regulated by adenosine. The presence of adenosine receptors on photoreceptors and the physiological evidence that endogenous adenosine is inhibitory at the rod synapse raises the possibility that cones might also be modulated by adenosine.

The present study is driven by evidence that cones, like rods, use dihydropyridine (DHP)-sensitive L-type Ca^{2+} channels to control release of the neurotransmitter L-glutamate (Wilkinson and Barnes, 1996; Thoreson et al., 1997) and that adenosine inhibits the Ca^{2+}-activated chloride current in cones (Barnes and Hille, 1989), suggesting that adenosine likely modulates cone Ca^{2+} channels. To explore the presynaptic role of adenosine at the cones, we tested the effects of adenosine on voltage-dependent Ca^{2+} channels from cones in the salamander retina. The effects of adenosine on I_{Ca} and depolarization-evoked Ca^{2+} increases were studied by using Ca^{2+} imaging and electrophysiological techniques. Our results indicate that adenosine inhibits the calcium current (I_{Ca}) and depolarization-evoked Ca^{2+} influx in a concentration-dependent manner in cones of the tiger salamander retina. This study provides evidence that, as in rods, adenosine can inhibit voltage-dependent Ca^{2+} influx into the terminals of cones, which likely suppresses transmitter release, suggesting that adenosine functions as an inhibitory transmitter at the first synapse in visual processing.

MATERIALS AND METHODS

Tissue Preparation and Retinal Slices

Larval tiger salamanders (*Ambystoma tigrinum*; Kons, Germantown, WI, or Charles Sullivan, TN; 7–10 in.) were cared for according to ARC institutional guidelines set forth at UCLA. The retinal slice preparation is similar to that developed by Werblin (1978) and described in detail by Wu (1987). Briefly, larval tiger salamanders were sacrificed by decapitation and rapidly pithed, the eyes were enucleated, and the anterior portion of an eye including the lens was removed. The resulting eyecup was cut into quarters and a section placed vitreal side down on a piece of filter paper (Millipore; 2 × 5 mm, type GS, 0.2-μm pores). After the retina had adhered to the filter paper, it was isolated under chilled amphibian superfusate. The retina and filter paper were cut into 150–200-μm slices using a tissue chopper (Stoelting Tissue Slicer, Stoelting Co., Wood Dale, IL) mounted with a single side of a double-edged razor blade (No. 121-6; Ted Pella Inc., Redding, CA). Slices were

rotated 90° to permit viewing of the retinal layers when placed under a water-immersion objective (Zeiss ×40, 0.8 NA, or ×63, 0.95 NA) and viewed on an upright, fixed-stage microscope (Zeiss Axioskop FS2; Zeiss, Thornwood, NY).

Isolated Photoreceptors

Retinas from two eyes were isolated in a chilled low-Ca^{2+} Mg^{2+}-free solution consisting of (in mM): 111 NaCl, 0.5 $CaCl_2$, 2.5 KCl, 10 HEPES, 5 glucose (pH 7.8). The eyecup was cut into quarters, and the retinal pieces were transferred to a low-Ca^{2+} solution containing papain (10.0–12.0 U/ml; Worthington Biochemical Inc., Lakewood, NJ) activated by D,L-cysteine (pH 7.4). Retinas were incubated for 35 min at 25–30°C and gently agitated on a stirrer. Retinas were then washed three times with a chilled incubation solution containing (in mM): 111 NaCl, 2.5 KCl, 1.8 $CaCl_2$, 0.5 $MgCl_2$, 10 HEPES, 5 glucose, 10 ascorbic acid, 7.5 mg/ml bovine serum albumin (BSA), and DNase 50 U/ml (Worthington Biochemical Inc.). Retinas were gently triturated in this solution, and the resulting cell suspension was plated on coverslips previously coated with 1 mg/ml concanavalin A (Con A). Superfusion was begun after letting cells settle and attach for 10–15 min at 6–8°C.

Solutions and Perfusion

Solutions were delivered to the perfusion chamber at a rate of 1 ml/min by using a single-pass, gravity-feed perfusion system. Drugs were typically bath applied. The normal amphibian superfusate contains (in mM): 111 NaCl, 2.5 KCl, 2 $CaCl_2$, 0.5 $MgCl_2$, 10 HEPES, and 5 glucose. The pH of all solutions was adjusted to 7.8 with NaOH and the osmolarity adjusted if necessary to 245 ± 5 mOsm. Solutions were continuously bubbled with 100% O_2. During recordings of I_{Ca}, the following solution was used (in mM): 91 NaCl, 2.5 CsCl, 10 $BaCl_2$, 0.5 $MgCl_2$, 10 HEPES, 5 glucose, 0.1–0.3 niflumic acid, and 0.1 picrotoxin.

Electrophysiology

Patch pipettes were pulled on a Narashige PP-830 vertical puller from borosilicate glass pipettes (1.2 mm O.D., 0.9 mm I.D., omega dot; WPI, Sarasota, FL). We used the perforated-patch method of whole-cell recording with the poreforming antibiotic nystatin (Rae et al., 1991). For successful sealing when using antibiotic solutions, pipettes with tips of ~1 μm O.D. and resistances of 8–15 MΩ were typically used. The pipette electrolyte solution contained (in mM): 54 KCl, 61.5 KCH_3SO_4, 3.5 $NaCH_3SO_4$, 10 HEPES. For recording of I_{Ca}, KCl was replaced by CsCl and KCH_3SO_4 by $CsCH_3SO_3$. The pH was adjusted to 7.2 with KOH or CsOH, and the osmolarity was adjusted if necessary to 245 ± 5 mOsm. Nystatin was mixed in dimethylsulfoxide (DMSO) at a concentration of 120 mg/ml, vortexed briefly, and then added to the pipette electrolyte solution to achieve a final concentration of 480 μg/ml. Fresh antibiotic solutions were made every 3 hr. In successful recordings, seals greater than 1 GΩ were usually obtained in 30 sec or less, and cells are usually fully perforated with whole-cell access within 5 min of sealing. After perforation, access resistance generally fell to <40 MΩ with stable recordings of I_{Ca}. A voltage ramp protocol was used for measurements of I_{Ca}. Comparisons between steady-state measurements of I_{Ca} made with a voltage step protocol (150-msec steps) and a ramp protocol (0.5 mV/msec) suggested that amplitude or midpoint measurements of I_{Ca} are not significantly altered by use of a ramp protocol (see Fig. 1A). Cones in which capacitative transients could not be fit by single exponentials were excluded from analysis. Currents were acquired and analyzed in PClamp 8.0 software (Molecular Devices, Sunnyvale, CA). For measurements of I_{Ca} in cones, the leak conductance was assumed to be ohmic and equal to the minimum conductance between −75 and −55 mV, then was digitally subtracted.

Measurement of Ca^{2+} Transients

Intracellular Ca^{2+} changes were assessed by using the calcium-sensitive dye fluo-4 on isolated cones. Fluo-4/AM (Molecular Probes, Eugene, OR) was prepared as a 1 mM stock solution in DMSO and diluted in mammalian superfusate to a final concentration of 0.5 μM. Cells were incubated in fluo-4 for 15 min at 5–8°C. Loading of cells for longer times or at higher concentrations of fluo-4 resulted in overloading of the calcium indicator dye. This presumably chelated most of the free Ca^{2+} (fluo-4 K_d ~ 380 nM) or generated high levels of aldehydes upon cleavage of the acetomethyl portion (AM) of the dye, resulting in toxicity to the cells and an inability to respond to a stimulus that should generate a Ca^{2+} transient. Images were collected with a Zeiss 510 META LSM or LSM 5 Pascal mounted to an upright microscope (Zeiss Axioplan 2 or Axioskop FS2) equipped with a Axoplan ×63 (NA 0.95) water-immersion objective. A 488-nm laser line from an argon laser provided excitation of the sample, and the emission was collected through a 505-nm LP filter and collected on a photomultiplier tube. Additional magnification, time series, and background subtraction were controlled by Zeiss LSM acquisition software. All images were acquired as 12 bit. To activate voltage-dependent Ca^{2+} channels, cells were depolarized by increasing $[K^+]_o$ from 2.5 to 50 mM for 1 min. Images were acquired at 5–10-sec intervals, and the interval times were decreased during elevated $[K^+]_o$ applications. For analysis, a region of interest was drawn over the terminal, and the change in fluorescence was interpreted as reflecting changes in $[Ca^{2+}]_i$. For cones, the terminal was defined as the broad synaptic-vesicle-filled extension located under the soma (Mandell et al., 1993; Sherry et al., 1998, 2001). The change produced in the presence of the test solution was compared with the averaged baseline measurements, which consists of three measurements prior to the application of the drug or stimulus. Values for control conditions were determined by averaging the prior control and subsequent wash responses for each drug application. Typically, one or two cells can be analyzed on each coverslip, and all experiments were performed on at least three different preparations. Statistical analysis was performed via Student's *t*-test (GraphPad Prism 4.0). In the case of multiple comparisons, a one-way ANOVA in conjunction with the Newman-Keuls post hoc test was applied. To determine the EC_{50}, the concentration required to produce a half-maximal inhibition of the K^+-evoked Ca^{2+} increase in the presence of adenosine, the data were fit to a theoretical sigmoidal binding equation: $B/B_{max} = [1 + (c/EC_{50})^h]^{-1}$, where c is the concentration of adenosine tested, h is the Hill coefficient, and B/B_{max} is the fractional normalized response or percentage inhibition of adenosine at the specific concentration tested.

Immunohistochemistry

Eyecups and isolated cells were fixed with 2% or 4% paraformaldehyde (PFA) in 0.1 M phosphate buffer (PB; pH 7.4) for 20 min to 1.5 hr at room temperature. Mouse anti-VAMP1 antibody (Cat. No. 104 001, clone Cl 10.1) was acquired from Synaptic Systems (Göttingen, Germany). Anti-VAMP was used at dilutions of 1:500–1:2,000. Rabbit anti-piccolo antibody (catalog No. 142 002) was acquired from Synaptic Systems. Anti-piccolo was used at a dilution of 1:20,000. All tissue and cells were labeled using the indirect fluorescence technique (Sassoe-Pognetto, et al., 1994). The location of the primary antibody/antigen complex was detected by using secondary antibodies conjugated to either goat anti-mouse Alexa 488 (for VAMP) or goat anti-rabbit Alexa 568 (for piccolo; Molecular Probes). All secondary antibodies were used at dilutions of 1:1,000. Retinal sections or coverslips were washed after each incubation with either primary or secondary antibody with 0.1 M PB to remove any unbound primary or secondary antibody. To check for antibody specificity, controls were prepared by omitting the primary antibody during the incubation. In this case, only the immunoreactivity for the nonspecific background staining from the secondary antibody was detected.

Loading of Synaptored-C2 (FM 4-64) in Retinal Slices and Isolated Cells

Synaptored-C2 (Biotium Inc., Hayward, CA) is an activity-dependent dye with the same physiochemical properties as FM 4-64 and can be used to monitor exocytosis from neurons (Ryan, 2001; Brager et al., 2003). After removal of the eyes as described above and prior to papain enzyme treatment, the eyecups were incubated in 40 μM Synaptored-C2 for 15 min in the dark. The retinas were then washed three times in chilled Ca^{2+}-free or low-Ca^{2+} (0.5 mM) superfusate containing ADVASEP-7 (Biotium Inc.; 500 μM), a cyclodextran that chelates Synaptored-C2 and aids in the removal of excess membrane associated dye (Kay et al., 1999). For retinal slices, Synaptored-C2-loaded retinas were exposed to bright ambient room light to hyperpolarize photoreceptors and placed in low-Ca^{2+} (0.5 mM) amphibian superfusate during slicing to prevent dye unloading. Dissociated cells were plated onto Con A-coated coverslips as described above. Synaptored-C2 dye was excited using the 488-nm laser line, and emitted light was collected through a 650-nm LP filter.

Drugs Solutions

Adenosine was obtained from Sigma (St. Louis, MO). Adenosine was prepared fresh at the final concentration or from a 50 mM stock in DMSO. Superfusion with 0.1% DMSO alone was not found to affect any of the properties of I_{Ca} or Ca^{2+} imaging responses that we studied.

RESULTS

Adenosine Inhibits Cone I_{Ca}

To determine whether Ca^{2+} entry through cone Ca^{2+} channels is suppressed in the presence of adenosine, we measured I_{Ca} in cones in retinal slices by using the perforated-patch clamp whole-cell recording technique (Rae et al., 1991). Voltage ramps were applied using the protocol shown in Figure 1A. Cells were held at −70 mV, and the voltage was ramped from −90 mV to +60 mV over 300 msec. In these experiments, we refer to the inward current evoked by a depolarizing voltage ramp in the presence of 10 mM Ba^{2+} as I_{Ca}. The slowly developing, U-shaped current-voltage relationship usually appeared at or above −45 mV and peaked between −10 and 0 mV and then diminished at more positive potentials.

Based on previous studies on rod photoreceptors (Stella et al., 2002, 2003) and experiments on other neuronal preparations (Delaney and Geiger, 1998; Dale et al., 2000), a concentration of adenosine was applied that would adequately activate adenosine receptors on cones. Because adenosine receptors generally require up to micromolar concentrations for activation (Dunwiddie and Diao, 1994; Delaney and Geiger, 1998; Fredholm et al., 2001), a relatively modest concentration of adenosine was tested on cones. The effect of adenosine (50 μM) on a small single cone I_{Ca} is shown in Figure 1B. Figure 1B illustrates current-voltage profiles of I_{Ca} in control/wash conditions (Fig. 1B, traces 1 and 3) and in the presence of adenosine (Fig. 1B, trace 2). Figure 1C plots the peak amplitude of I_{Ca} measured with voltage ramps every 30 sec. Inhibition of the cone I_{Ca} began within 30–60 sec, the time required for complete solution exchange in the recording chamber. Full inhibition was observed after 2 min, and current amplitudes recovered after ~5 min washout of adenosine. This time course is similar to the effects of adenosine previously reported for I_{Ca} from rod photoreceptors (Stella et al., 2002).

All cone subtypes responded to adenosine; however, we observed that some cells regardless of the cone subtype had little or no inhibition. This has been observed in rod photoreceptors in the slice. In rod photoreceptors, adenosine failed to inhibit depolarization-evoked $[Ca^{2+}]_i$ increases significantly in some cells. However, blockade of Ca^{2+}-induced Ca^{2+} release (CICR) with ryanodine restored the ability of adenosine to inhibit K^+-evoked $[Ca^{2+}]_i$

increases in rods (Stella et al., 2003). This is attributed to the ability of CICR to alter Ca^{2+} homeostasis and transmitter release in rods (Krizaj et al., 1999, 2003). However, it does not appear that CICR plays a significant role in modulating Ca^{2+} homeostasis in cones, because CICR is only unmasked in the presence of inhibitors of the plasma membrane Ca^{2+} ATPases (PMCAs) and mitochondrial Ca^{2+} sequestration (Krizaj et al., 2003). Blockade of these two homeostatic Ca^{2+} mechanisms was not applied in these experiments, so it is more likely that endogenously released adenosine might obscure the effects of exogenously applied adenosine on cone photoreceptors in the slice (Ribelaya and Mangel, 2005; Stella et al., 2003). Therefore, for these experiments, we excluded cells in which adenosine (50 μM) inhibited I_{Ca} by less than 10% and performed the remainder of the experiments described in this study on isolated cones from tiger salamander retina. The mean reduction in cone I_{Ca} was 39.5% ± 8.0% (n = 8, $P = 0.009$).

Morphological Identification of Synaptic Terminals in Rods and Cones of the Tiger Salamander Retina

To study Ca^{2+} changes in terminals of isolated photoreceptors, it is necessary to map the terminal region of these cells. The morphology of rod synaptic terminals is very different from that of cone synaptic terminals in the tiger salamander retina. Rods contain one or more thin axons, each of which terminates in a large synaptic terminal within the outer plexiform layer (OPL; Fig. 2). Salamander cones have somata that are positioned closer to the OPL but do not possess an axon-like processes but form a broad synaptic-vesicle-filled extension in the OPL (Mandell et al., 1993; Sherry et al., 1998, 2001). This can be observed in Figure 2, which shows immunoreactivity for synaptic proteins, VAMP and piccolo. VAMP, also known as *synaptobrevin*, is a key component of the core complex needed for docking and fusion of synaptic vesicles with the presynaptic plasma membrane. VAMP labeling was present in the OPL and inner plexiform layer (IPL; Fig. 2A) and was especially prominent in rod and cone terminals. Immunoreactivity for VAMP was distributed throughout the terminals of double cones, large single cones, and small single cones (Fig. 2B–D). Piccolo is a cytomatrix protein that was first identified at conventional synapses in brain (Garner et al., 2000). Piccolo is associated with the synaptic ribbon and is in the adjacent cytoplasm (Dick et al., 2001). Similar to VAMP, piccolo labeled both the OPL and the IPL (Fig. 2E). As expected, piccolo labeled structures in the terminals of isolated rods and cones and was restricted solely to the synaptic terminal region (Fig. 3F–I). Surprisingly, piccolo did not label discrete structures tightly associated with the synaptic ribbon in photoreceptor terminals (Dick et al., 2001); instead, piccolo labeling was diffuse throughout the entire salamander photoreceptor terminal (Fig. 3F–I). Ruling out fixation conditions and antibody specificity, this observed difference could be due to unique spatial expression of piccolo throughout salamander photoreceptor terminals, which may have important implications for ribbon targeting and synaptic vesicle release; however, a more extensive investigation is necessary to address this issue, which is beyond the scope of this study.

Additional evidence that synaptic terminals in cones are broad, vesicle-filled cytoplasmic extensions within the OPL and isolated cells comes from loading of the activity-dependent dye Synaptored-C2. Synaptored-C2 labels recycling vesicles as they internalize the dye at the plasma membrane during periods of activity. After washing out the surface-bound probe, the recycling vesicle pool is easily visualized. This allows for simple synapse identification in a living preparation and provides quantitative information about recycling pools of vesicles (Ryan, 2001). Figure 3A–D shows that Synaptored-C2 labeling is in accordance with the piccolo and VAMP immunolabeling and previous studies mapping the site of the synaptic terminals in cone subtypes of the tiger salamander retina (Sherry et al., 2001).

Characterization of Depolarization-Evoked Ca^{2+} Increases in Photoreceptor Terminals

To demonstrate the difference in the spatial and temporal kinetics of Ca^{2+} entry into the synaptic terminal and soma of rods and cones, spatially averaged Ca^{2+} signals were measured with fluo-4 AM-loaded photoreceptors. In every cell, a region of interest was drawn around the perikaryal region of the inner segment comprising the cell nucleus and the surrounding cytoplasm and the synaptic terminal region of the cell. To monitor the differences in the spatiotemporal responses of isolated rods and cones in salamander retina to a depolarization-evoked stimulus, cells were superfused with elevated $[K^+]_o$ (2.5 mM to 50 mM). This K^+-evoked depolarization is a strong depolarization and generally increases the membrane potential to a more positive potential of about −10 mV, resulting in an increase of $[Ca^{2+}]_i$ near 350 nM (Thoreson et al., 2003).

Figures 4A illustrates the response of an isolated rod photoreceptor to elevated $[K^+]_o$ (50 mM); $[Ca^{2+}]_i$ levels rose rapidly upon depolarization in the terminal and preceded any increase in the soma and then returned to prestimulus levels following washout of elevated $[K^+]_o$. Conversely, application of the elevated $[K^+]_o$ (50 mM) to an isolated double cone photoreceptor generated a simultaneous increase in terminal and somatic $[Ca^{2+}]_i$ regions of both the principal and the accessory double cone members (Fig. 4B). Similar responses were also observed in small single and large single cones (data not shown). Strikingly, these sequential images show that depolarization-evoked Ca^{2+} increases in the synaptic region of cones are very different from those of rods. This is due to the fact that the cone terminal has a broad synaptic-vesicle-filled extension located under the soma and not compartmentalized like the terminals of rods (i.e., both compartments are separated by a long thin fiber emanating from the spherical inner segment; see Figs. 2, 3).

Adenosine Inhibits Depolarization-Evoked Ca^{2+} Increases in Cone Terminals

We had established the location of the synaptic terminal region of salamander cones (see Figs. 2–4), so we were confident that we could accurately monitor terminal changes in cone Ca^{2+} levels via confocal microscopy. Ca^{2+}-imaging experiments were performed on isolated cones to test whether adenosine reduced depolarization-evoked $[Ca^{2+}]_i$ increases in cone photoreceptors. Because cone I_{Ca} is inhibited by adenosine, we expected that adenosine would inhibit K^+-evoked Ca^{2+} entry into cone terminals. Figure 5 shows a plot of the $[Ca^{2+}]_i$ response measured in a double cone photoreceptor before, during, and after the application of adenosine (50 μM). Corresponding pseudocolor images of fluorescence from the same cell are displayed in Figure 5B, showing cells in normal (2.5 mM), elevated (50 mM) $[K^+]_o$ superfusate, and elevated (50 mM) $[K^+]_o$ amphibian superfusate in the presence of adenosine (50 μM). Adenosine produced a reversible inhibition of the depolarization-evoked $[Ca^{2+}]_i$ increase. Adenosine also inhibited depolarization-evoked $[Ca^{2+}]_i$ increases in large single (Fig. 5C) and small single cones (Fig. 5D). On average, adenosine (50 μM) caused a −45.1% ± 8.1% (n = 8, $P = 0.009$) reduction in the K^+-evoked fluorescence change in cone photoreceptors. Significant inhibition of the K^+-evoked $[Ca^{2+}]_i$ increase was seen at concentrations as low as 10 μM (−25.0 ± 8.7%, n = 5, $P = 0.0168$), and inhibition increased in a concentration-dependent manner with concentrations ≤50 μM (Fig. 6). The inhibition was concentration dependent (Fig. 6), with an EC_{50} value of 15.6 μM.

DISCUSSION

Our results reveal an inhibitory role for adenosine at the cones, indicating that adenosine inhibits voltage-dependent Ca^{2+} channels, which should suppress release of L-glutamate by inhibiting depolarization-evoked Ca^{2+} influx in cones. The adenosine-mediated inhibition of I_{Ca} and depolarization-evoked Ca^{2+} influx in cone terminals appears to be due to activation of presynaptic adenosine receptors present on cones. As considered further below, the

inhibitory action of adenosine at cones is similar to that of rods and suggests that adenosine functions as an important inhibitory transmitter in the outer retina to suppress glutamate release from photoreceptors onto second-order neurons. Thus, adenosine likely regulates the synaptic release of L-glutamate from cones in the outer retina.

Adenosine as an Inhibitory Transmitter at Photoreceptors in the Outer Retina

Adenosine has been shown previously to inhibit the Ca^{2+}-activated chloride current ($I_{Cl(Ca)}$) in cones from tiger salamander retina (Barnes and Hille, 1989). We found that adenosine inhibited I_{Ca} and depolarization-evoked Ca^{2+} increases in cone terminals of the tiger salamander retina in a concentration-dependent manner, with an EC_{50} of 15.6 μM (Figs. 2B,C, 5, 6). The observed effects of adenosine on cones are analogous to the adenosine-mediated inhibition observed in rods in the tiger salamander retina (Stella et al., 2002). In this study, we did not address the pharmacological subtype of receptor mediating these effects on cones. However, we speculate that some cone subtypes use different adenosine receptors than rods (A_{2A}-like receptor). Support for this comes from previous observations examining the effect of activators (forskolin, Sp-cAMP) and inhibitors (Rp-cAMP) of PKA on rod and cone I_{Ca} (Stella and Thoreson, 2000). Rod and small single cone I_{Ca} are suppressed in the presence of increased cAMP or PKA activity, whereas large single cone and double cone I_{Ca} are enhanced in the presence increased cAMP or PKA activity. Adenosine receptors are classified into four molecular and pharmacological subtypes: A_1, A_{2A}, A_{2B}, and A_3. Adenosine receptors couple to different intracellular effectors (e.g., PKA and IP_3). A_1 and A_3 receptor activation either inhibits a PKA-dependent pathway or stimulates PLC activity and releases Ca^{2+} from intracellular stores (Dunwiddie and Masino, 2001). A_{2A} receptors couple positively to the cAMP-dependent PKA pathway, and A_{2B} couples to IP_3 and cAMP-dependent PKA pathways (Dunwiddie and Masino, 2001; Ralevic and Burnstock, 1998). Insofar as Ca^{2+} channels in cone sub-types are inhibited by adenosine but respond differently to cAMP stimulation or PKA activity, it is possible that small single cones would contain A_2-like receptors, whereas large single cones and double cones might utilize a different adenosine receptor subtype to inhibit Ca^{2+} channels (A_1 or A_3 receptor); however, a more detailed pharmacological study is needed to clarify this issue.

Adenosine's role as a presynaptic inhibitory transmitter at the photoreceptor synapse is strongly supported by the following evidence. 1) Adenosine inhibits voltage-dependent Ca^{2+} influx in both rod (Stella et al., 2002) and cone terminals (Figs. 1B,C, 5, 6). 2) Adenosine inhibits transmitter release from rods onto second-order neurons (Stella et al., 2003). 3) The ability of ZM-241385 alone, the A_{2A}-selective antagonist, to enhance transmitter release from rods in dark-adapted retina (Stella et al., 2003) suggests that endogenous adenosine is likely present in higher concentrations in the outer retina under dark conditions. This observation also explains why the effects of exogenously applied adenosine could be masked in dark-adapted retinal slices, and consistent with reports indicating that extracellular levels of adenosine are controlled directly by the environmental levels of illumination or lighting conditions (Ribelaya and Mangel, 2005).

The finding that adenosine can alter glutamatergic transmission is not unique to the outer retina; adenosine can also alter both glutamate-induced and voltage-dependent Ca^{2+} entry into ganglion cells through activation of A_1 adenosine receptors (Hartwick et al., 2004). Generally, A_1 receptor activation contributes to tonic suppression of glutametergic transmission in the CNS (Yawo and Chuhma, 1993; Mogul et al., 1993; Wu and Saggau, 1994; Dunwiddie and Masino, 2001). This results in a marked depression of neuronal activity. Similar to adenosine's inhibitory action on photoreceptors, adenosine reduces the excitability in ganglion cells by decreasing Ca^{2+} entry. One major difference between photoreceptors and ganglion cells is that adenosine's inhibitory effects on ganglion cells were mediated by A_1 adenosine receptors (Hartwick et al., 2004), unlike the case in rods,

where activation of an A_2-like receptor suppressed voltage-dependent Ca^{2+} influx (Stella et al., 2002, 2003). Despite these differences in signaling pathways and receptor systems, it is possible that the role is likely the same. Activation of adenosine receptors would dampen the excitatory output of photoreceptors and ganglion cells serving as a tight feedback mechanism regulated by light (Ribelaya and Mangel, 2005) to control the flow of visual information to the brain. More importantly, extracellular adenosine levels increase after ischemia or excitotoxic insults (Ghiardi et al., 1999; Li and Roth, 1999), suggesting that adenosine may also play a neuroprotective role in photoreceptors and ganglion cells by protecting them from damage and provide a way to limit retinal insult in ischemia and neurodegenerative diseases (e.g., glaucoma).

Sources of Adenosine in the Outer Retina

Adenosine levels are highly linked to energy supply and demand and reflect an equilibrium between the processes that lead to the appearance of adenosine (e.g., formation of adenine nucleotides by nucleotidases and transport) and mechanisms that reduce adenosine levels (e.g., uptake or enzymatic breakdown to inosine; Gu and Geiger, 1992; Roth et al., 1997). Adenosine levels formed from ATP have been hypothesized to be under dual control in order to maintain the extracellular level of adenosine either by light/dark adaptation or by a circadian clock in the retina (Ribelaya and Mangel, 2005). Under constant-dark conditions, extracellular adenosine is likely synthesized from ATP released by cells via the sequential actions of the ecto-ATPase and the ectonucleotidase (ectoNTase; Newman, 2003, 2005; Ribelaya and Mangel, 2005). However, the exact mechanisms governing adenosine release and metabolism have not been elucidated in the retina.

As mentioned above, one likely way in which adenosine formation occurs is through metabolism of ATP. One source could be derived from photoreceptors themselves; in the dark, photoreceptors are more metabolically active, and higher ATP turnover occurs through the activity of Na^+/K^+ ATPase in the photoreceptor inner segment to counter the steady influx of Na^+ entering though cyclic nucleotide-gated channels in the outer segment. Thus, the increased ATP turnover can elevate intracellular levels of adenine nucleotides, which can be transported or released into the extracellular space and subsequently degraded into adenosine by extracellular ectonucleotidases. This hypothesis is supported by the finding that application of analogues that compete with ATP and adenine nucleotides (GMP, αβmADP, or ARL67156) decrease the formation of extracellular adenosine under both light and dark conditions, suggesting that adenosine is formed extracellularly from released or transported ATP or adenine nucleotides (Ribelaya and Mangel, 2005). In this way, adenosine levels could tightly regulate transmitter release from photoreceptors by feeding back onto rods and cones and suppressing L-glutamate release in the dark.

Other sources that could provide sufficient amounts of ATP that could be metabolized into adenosine in the outer retina include retinal pigmented epithelial (RPE) cells and Müller cells. RPE cells have been shown to release ATP through hemichannels during development (Pearson et al., 2005), and it is likely that ATP released from the RPE cells can easily reach the photoreceptors. Müller glial cells have processes that span the entire retina, and it is conceivable that ATP released from these cells (Newman, 2003, 2005) could reach the OPL and act on adenosine receptors present on rods and cones.

Physiological Significance

There is clearly a link in the retina between the metabolic state of the retina, ATP, adenosine levels, environmental lighting, and transmitter release at the first synapse in visual processing. It is clear from studies on adenosine levels under light or dark conditions that subtle changes in illumination could be accompanied by changing levels of adenosine (Perez

et al., 1986; Paes de Carvalho et al., 1990; Blazanski and Perez, 1991; Ribelaya and Mangel, 2005), which can have a direct impact on transmitter release from photoreceptors. Adenosine-mediated feedback limiting L-glutamate release has been described for the CNS (Brambilla et al., 2005). This mechanism utilizes activation of presynaptic A_1 adenosine receptors by increasing extracellular adenosine in a N-methyl-D-aspartate receptor-dependent manner. This increase in adenosine was found to be sufficient to feedback onto presynaptic terminals and limit L-glutamate release. In contrast, the effects of adenosine in the retina are likely mediated by different adenosine receptors on rods and cones. Support for this hypothesis comes from the fact that adenosine receptors use the cAMP-dependant pathway to transduce their signals (Dunwiddie and Masino, 2001), and rod and cone Ca^{2+} channels respond differently to cAMP activity (a more detailed discussion is provided by Stella and Thoreson, 2000). Thus, the control of adenosine levels by both the metabolic state of the retina and the environmental lighting conditions suggests that, under dark conditions, released adenosine would act tonically to inhibit transmitter release from both cones and rods in the outer retina. This negative feedback mechanism by adenosine on rods and cones may function like a tonic brake that can limit the amount of L-glutamate released from photoreceptors in the dark- or dark-adapted state in the outer retina and have a profound impact on inputs into second-order neurons.

Acknowledgments

N.C.B. is a VA Senior Career Scientist. W.D.H. was supported by a Fight-For-Sight Student Fellowship, a Jeanette Duval Scholarship, and the UCLA Undergraduate Research Scholars Program. Pilot experiments for these studies were first performed when S.L.S. was at the University of Nebraska Medical Center. S.L.S. thanks Dr. Wallace B. Thoreson at University of Nebraska Medical Center for his support, guidance, and generosity. The authors also thank Dr. Arlene Hirano for reading the manuscript and providing insightful comments.

Contract grant sponsor: National Institutes of Health; Contract grant number: EY 04067; Contract grant number: EY 15573; Contract grant number: DK 41301; Contract grant sponsor: U.S. Department of Veterans Affairs (to N.C.B.); Contract grant sponsor: Fight for Sight; Contract grant number: GA05039 (to S.L.S.).

REFERENCES

Barnes S, Hille B. Ionic channels of the inner segment of tiger salamander cone photoreceptors. J Gen Physiol. 1989; 94:719–743. [PubMed: 2482325]

Blazynski C. Discrete distributions of adenosine receptors in mammalian retina. J Neurochem. 1990; 54:648–655. [PubMed: 2299359]

Blazynski C, Perez MT. Adenosine in vertebrate retina: localization, receptor characterization, and function. Cell Mol Neurobiol. 1991; 11:463–484. [PubMed: 1683815]

Blazynski C, Mosinger JL, Cohen AI. Comparison of adenosine uptake and endogenous adenosine-containing cells in mammalian retina. Vis Neurosci. 1989; 2:109–116. [PubMed: 2487641]

Braas KM, Zarbin MA, Snyder SH. Endogenous adenosine and adenosine receptors localized to ganglion cells of the retina. Proc Natl Acad Sci U S A. 1987; 84:3906–3910. [PubMed: 3473489]

Brager DH, Luther PW, Erdelyi F, Szabo G, Alger BE. Regulation of exocytosis from single visualized GABAergic boutons in hippocampal slices. J Neurosci. 2003; 23:10475–10486. [PubMed: 14627631]

Brambilla D, Chapman D, Greene R. Adenosine mediation of presynaptic feedback inhibition of glutamate release. Neuron. 2005; 46:275–283. [PubMed: 15848805]

Dale N, Pearson T, Frenguelli BG. Direct measurement of adenosine release during hypoxia in the CA1 region of the rat hippocampal slice. J Physiol. 2000; 526:143–155. [PubMed: 10878107]

Delaney SM, Geiger JD. Levels of endogenous adenosine in rat striatum. II. Regulation of basal and N-methyl-D-aspartate-induced levels by inhibitors of adenosine transport and metabolism. J Pharmacol Exp Ther. 1998; 285:568–572. [PubMed: 9580599]

Dick O, Hack I, Altrock WD, Garner CC, Gundelfinger ED, Brandstatter JH. Localization of the presynaptic cytomatrix protein piccolo at ribbon and conventional synapses in the rat retina: comparison with bassoon. J Comp Neurol. 2001; 439:224–234. [PubMed: 11596050]

Dunwiddie TV, Diao L. Extracellular adenosine concentrations in hippocampal brain slices and the tonic inhibitory modulation of evoked excitatory responses. J Pharmacol Exp Ther. 1994; 268:537–545. [PubMed: 8113965]

Dunwiddie TV, Masino SA. The role and regulation of adenosine in the central nervous system. Annu Rev Neurosci. 2001; 24:31–55. [PubMed: 11283304]

Fredholm BB, IJzerman AP, Jacobson KA, Klotz KN, Linden J. International Union of Pharmacology. XXV. Nomenclature and classification of adenosine receptors. Pharmacol Rev. 2001; 53:527–552. [PubMed: 11734617]

Garner CC, Kindler S, Gundelfinger ED. Molecular determinants of presynaptic active zones. Curr Opin Neurobiol. 2000; 10:321–327. [PubMed: 10851173]

Ghiardi GJ, Gidday JM, Roth S. The purine nucleoside adenosine in retinal ischemia-reperfusion injury. Vis Res. 1999; 39:2519–2535. [PubMed: 10396621]

Gu JG, Geiger JD. Transport and metabolism of D-[^{3}H]adenosine and L-[^{3}H]adenosine in rat cerebral cortical synaptoneurosomes. J Neurochem. 1992; 58:1699–1705. [PubMed: 1560227]

Hartwick AT, Lalonde MR, Barnes S, Baldridge WH. Adenosine A1-receptor modulation of glutamate-induced calcium influx in rat retinal ganglion cells. Invest Ophthalmol Vis Sci. 2004; 45:3740–3748. [PubMed: 15452085]

Kay AR, Alfonso A, Alford S, Cline HT, Holgado AM, Sakmann B, Snitsarev VA, Stricker TP, Takahashi M, Wu LG. Imaging synaptic activity in intact brain and slices with FM1–43 in C. elegans, lamprey, and rat. Neuron. 1999; 24:809–817. [PubMed: 10624945]

Krizaj D, Bao JX, Schmitz Y, Witkovsky P, Copenhagen DR. Caffeine-sensitive calcium stores regulate synaptic transmission from retinal rod photoreceptors. J Neurosci. 1999; 19:7249–7261. [PubMed: 10460231]

Krizaj D, Lai FA, Copenhagen DR. Ryanodine stores and calcium regulation in the inner segments of salamander rods and cones. J Physiol. 2003; 547:761–774. [PubMed: 12562925]

Kvanta A, Seregard S, Sejersen S, Kull B, Fredholm BB. Localization of adenosine receptor messenger RNAs in the rat eye. Exp Eye Res. 1997; 65:595–602. [PubMed: 9367639]

Li B, Roth S. Retinal ischemic preconditioning in the rat: requirement for adenosine and repetitive induction. Invest Ophthalmol Vis Sci. 1999; 40:1200–1216. [PubMed: 10235554]

Mandell JW, MacLeish PR, Townes-Anderson E. Process outgrowth and synaptic varicosity formation by adult photoreceptors in vitro. J Neurosci. 1993; 13:3533–3548. [PubMed: 8340818]

Mogul DJ, Adams ME, Fox AP. Differential activation of adenosine receptors decreases N-type but potentiates P-type Ca^{2+} current in hippocampal CA3 neurons. Neuron. 1993; 10:327–334. [PubMed: 8382501]

Newman EA. Glial cell inhibition of neurons by release of ATP. J Neurosci. 2003; 23:1659–1666. [PubMed: 12629170]

Newman EA. Calcium increases in retinal glial cells evoked by light-induced neuronal activity. J Neurosci. 2005; 25:5502–5510. [PubMed: 15944378]

Paes de Carvalho R. Adenosine as a signaling molecule in the retina: biochemical and developmental aspects. An Acad Bras Cienc. 2002; 74:437–451. [PubMed: 12378312]

Paes de Carvalho R, Braas KM, Snyder SH, Adler R. Analysis of adenosine immunoreactivity, uptake, and release in purified cultures of developing chick embryo retinal neurons and photoreceptors. J Neurochem. 1990; 55:1603–1611. [PubMed: 2213012]

Pearson RA, Dale N, Llaudet E, Mobbs P. ATP released via gap junction hemichannels from the pigment epithelium regulates neural retinal progenitor proliferation. Neuron. 2005; 46:731–744. [PubMed: 15924860]

Perez MT, Ehinger BE, Lindstrom K, Fredholm BB. Release of endogenous and radioactive purines from the rabbit retina. Brain Res. 1986; 398:106–112. [PubMed: 3801882]

Rae J, Cooper K, Gates P, Watsky M. Low access resistance perforated patch recordings using amphotericin B. J Neurosci Methods. 1991; 37:15–26. [PubMed: 2072734]

Ralevic V, Burnstock G. Receptors for purines and pyrimidines. Pharmacol Rev. 1998; 50:413–492. [PubMed: 9755289]

Rey HL, Burnside B. Adenosine stimulates cone photoreceptor myoid elongation via an adenosine A2-like receptor. J Neurochem. 1999; 72:2345–2355. [PubMed: 10349843]

Ribelayga C, Mangel SC. A circadian clock and light/dark adaptation differentially regulate adenosine in the mammalian retina. J Neurosci. 2005; 25:215–22. [PubMed: 15634784]

Roth S, Rosenbaum PS, Osinski J, Park SS, Toledano AY, Li B, Moshfeghi AA. Ischemia induces significant changes in purine nucleoside concentration in the retina-choroid in rats. Exp Eye Res. 1997; 65:771–779. [PubMed: 9441700]

Ryan TA. Presynaptic imaging techniques. Curr Opin Neurobiol. 2001; 11:544–549. [PubMed: 11595486]

Sassoe-Pognetto M, Wassle H, Grunert U. Glycinergic synapses in the rod pathway of the rat retina: cone bipolar cells express the alpha 1subunit of the glycine receptor. J Neurosci. 1994; 14:5131–5146. [PubMed: 8046473]

Sherry DM, Bui DD, DeGrip WJ. Identification and distribution of photoreceptor subtypes in the neotenic tiger salamander retina. Vis Neurosci. 1998; 15:1175–1187. [PubMed: 9839981]

Sherry DM, Yang H, Standifer KM. Vesicle-associated membrane protein isoforms in the tiger salamander retina. J Comp Neurol. 2001; 431:424–436. [PubMed: 11223812]

Stella SL Jr, Thoreson WB. Differential modulation of rod and cone calcium currents in tiger salamander retina by D2 dopamine receptors and cAMP. Eur J Neurosci. 2000; 12:3537–3548. [PubMed: 11029623]

Stella SL Jr, Bryson EJ, Thoreson WB. A_2 adenosine receptors inhibit calcium influx through L-type calcium channels in rod photoreceptors of the salamander retina. J Neurophysiol. 2002; 87:351–360. [PubMed: 11784755]

Stella SL Jr, Bryson EJ, Cadetti L, Thoreson WB. Endogenous adenosine reduces glutamatergic output from rods through activation of A_2-like adenosine receptors. J Neurophysiol. 2003; 90:165–174. [PubMed: 12843308]

Studholme KM, Yazulla S. ^{3}H-adenosine uptake selectively labels rod horizontal cells in goldfish retina. Vis Neurosci. 1997; 14:207–212. [PubMed: 9147473]

Sun X, Barnes S, Baldridge WH. Adenosine inhibits calcium channel currents via A1 receptors on salamander retinal ganglion cells in a mini-slice preparation. J Neurochem. 2002; 81:550–556. [PubMed: 12065663]

Thoreson WB, Nitzan R, Miller RF. Reducing extracellular Cl^- suppresses dihydropyridine-sensitive Ca^{2+} currents and synaptic transmission in amphibian photoreceptors. J Neurophysiol. 1997; 77:2175–2190. [PubMed: 9114264]

Thoreson WB, Bryson EJ, Rabl K. Reciprocal interactions between calcium and chloride in rod photoreceptors. J Neurophysiol. 2003; 90:1747–1753. [PubMed: 12724369]

Werblin FS. Transmission along and between rods in the tiger salamander retina. J Physiol. 1978; 280:449–470. [PubMed: 211229]

Wilkinson MF, Barnes S. The dihydropyridine-sensitive calcium channel subtype in cone photoreceptors. J Gen Physiol. 1996; 107:621–630. [PubMed: 8740375]

Wu LG, Saggau P. Adenosine inhibits evoked synaptic transmission primarily by reducing presynaptic calcium influx in area CA1 of hippocampus. Neuron. 1994; 12:1139–1148. [PubMed: 8185949]

Wu SM. Synaptic connections between neurons in living slices of the larval tiger salamander retina. J Neurosci Methods. 1987; 20:139–149. [PubMed: 3037200]

Yawo H, Chuhma N. Preferential inhibition of omega-cenotoxin-sensitive presynaptic Ca^{2+} channels by adenosine autoreceptors. Nature. 1993; 365:256–258. [PubMed: 8396730]

Zhang C, Schmidt JT. Adenosine A1 and class II metabotropic glutamate receptors mediate shared presynaptic inhibition of retinotectal transmission. J Neurophysiol. 1999; 82:2947–2955. [PubMed: 10601431]

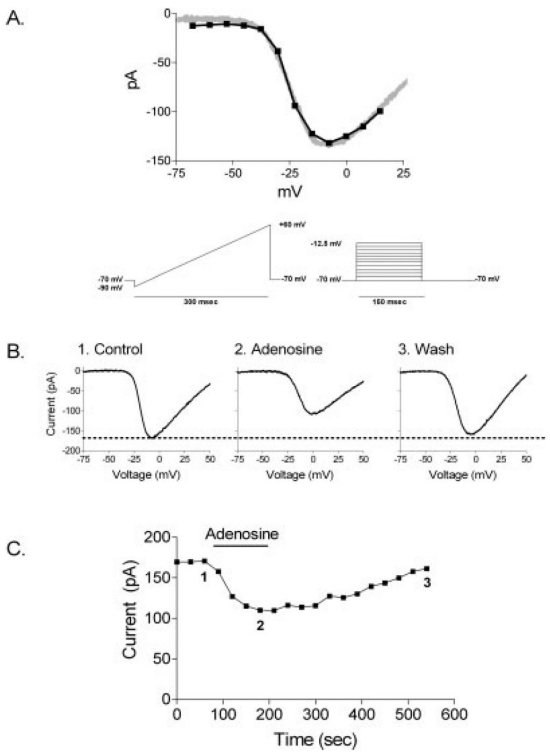

Fig. 1.

Adenosine (50 μM) inhibited small single cone I_{Ca}. **A:** Cone voltage ramp vs. voltage step: ramp (gray) 0.5 mV/msec vs. 150-msec voltage step protocol (black), each of the stimulus protocols is shown. **B:** The graph shows I–V relationships of voltage ramps obtained in control superfusate (1) and in the presence of 50 μM adenosine (2) and during the wash (3). **C:** The time course of adenosine-induced changes in the amplitude of I_{Ca} in a small single cone. Voltage ramps in B were obtained at time points 1 (control), 2 (adenosine), and 3 (wash). The cell was held at −70 mV.

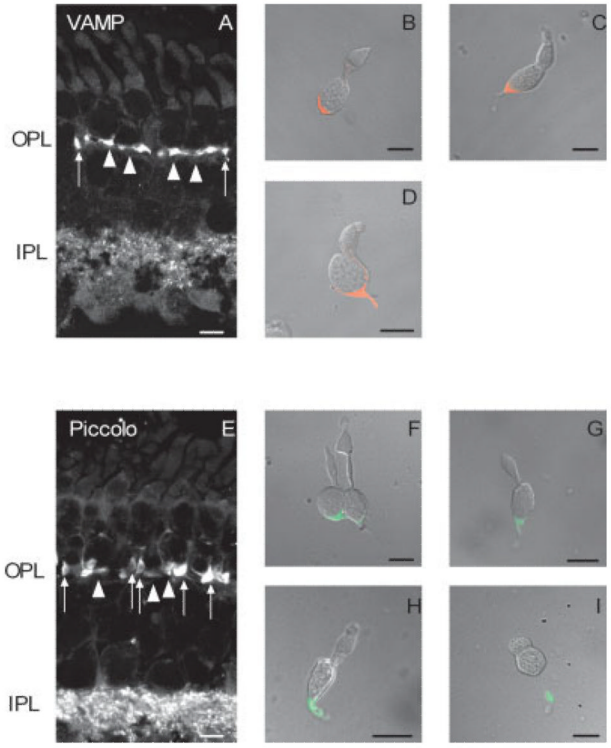

Fig. 2.

Confocal fluorescence images of tiger salamander retina immunostained with antisera against vesicle-associated membrane protein (VAMP) and piccolo. **A:** Image of a retinal section immunostained for VAMP. **B–D** show dissociated cones from the tiger salamander retina immunostained for VAMP. B: Accessory member of a double cone. C: Large single cone. D: Small single cone. VAMP immunofluorescence (red) is prominent in the synaptic terminals of rods (arrowheads) and cones (arrows) and in the IPL. **E:** Image of a retinal section immunostained for piccolo. **F–I** are dissociated photoreceptors from the tiger salamander retina immunostained for piccolo. F: Double cone. G: Large single cone without outer segment. **H:** Small single cone. **I:** Rod without an outer segment. Piccolo immunofluorescence (green), like that of VAMP, is prominent in the synaptic terminals of rods and cones, and in the IPL. No staining is observed in any of the cell layers. OPL, outer plexiform layer; IPL, inner plexiform layer. Goat anti-mouse IgG Alexa 488 was used to label anti-VAMP immunoreactivity, and goat anti-rabbit IgG Alexa 568 was used to label anti-piccolo immunoreactivity. Scale bars = 10 μm.

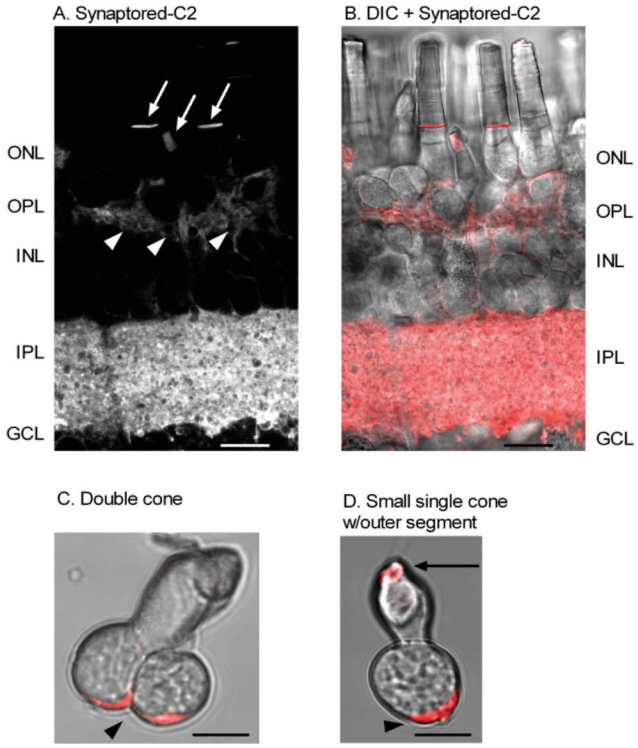

Fig. 3.

Activity-dependent dye (Synaptored-C2) loading in photoreceptor terminals of the tiger salamander retina. Synaptored-C2 activity-dependent labeling is restricted to terminal regions in the OPL and IPL of the retinal slice preparation. **A:** A living retinal slice loaded with 40 μM Synaptored-C2 for 15 min in the dark, then washed with ADVASEP-7 (500 μM). Arrowheads indicate synaptic loading of Synaptored-C2 into rod and cone terminals. Arrows indicate Synaptored-C2 dye uptake into outer segments of rods and cones. **B:** Combined brightfield differential interference contrast (DIC) image and Synaptored-C2 labeling of the retinal slice in A. **C:** Brightfield image of an isolated double cone loaded with Synaptored-C2 and then enzymatically dissociated with papain. **D:** Brightfield image of an isolated small single cone with outer segment loaded with Synaptored-C2 and then enzymatically dissociated with papain. In isolated cells, arrowheads indicate synaptic uptake of the activity-dependent dye, Synaptored-C2, and arrow indicates dye uptake into outer segment as seen in A and B of the retinal slice. Scale bars = 10 μm.

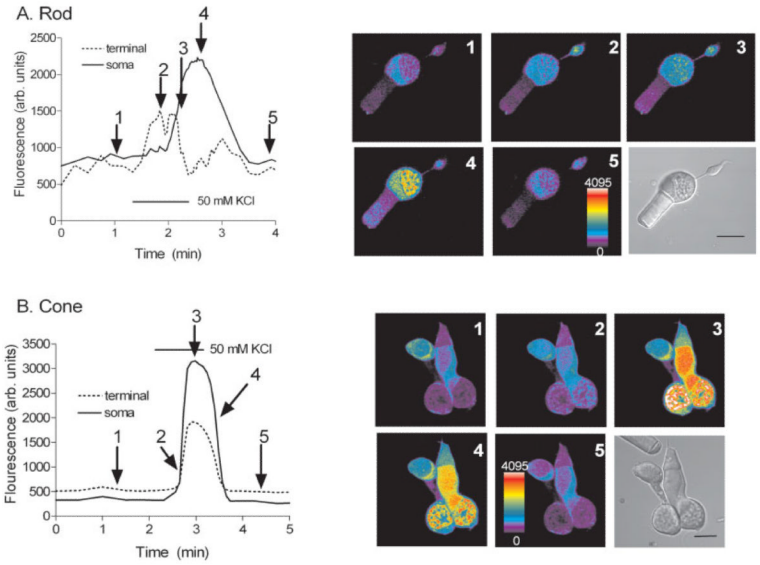

Fig. 4.

Comparison of the depolarization-evoked $[Ca^{2+}]_i$ increases in an isolated rod vs. an isolated cone. **A:** An isolated rod with corresponding pseudocolor images showing spatiotemporal $[Ca^{2+}]_i$ changes within different compartments to an elevated K^+ stimulus (50 mM). **B:** Isolated double cone with corresponding pseudocolor images showing the spatiotemporal $[Ca^{2+}]_i$ changes within different cellular compartments to an elevated K^+ stimulus. The arrows from the graphs at left point to corresponding time intervals of images shown at right. The rod in A: 1, control, prior to the stimulus application; 2, 20 sec after the stimulus application; 3, 40 sec after the stimulus application; 4, 1 min after the stimulus application; 5, wash. The cone in B: 1, control, prior to the stimulus application; 2, 5 sec after the stimulus application; 3, 40 sec after the stimulus application; 4, 1 min 10 sec after the stimulus application; 5, wash. Cells were stimulated with a 1-min application of elevated (50 mM) $[K^+]_o$. Scale bars = 10 μm.

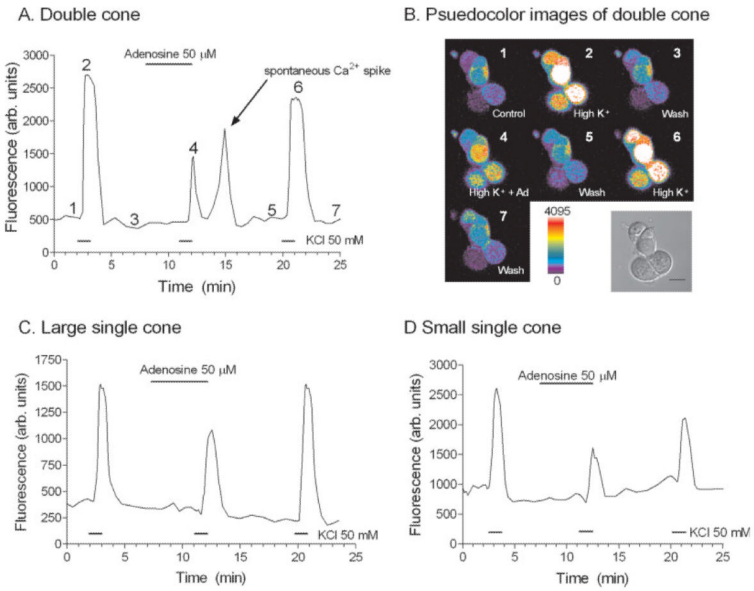

Fig. 5.

Adenosine inhibits the K^+-evoked-depolarization in terminals of isolated cone photoreceptors. **A:** A plot of $[Ca^{2+}]_i$ changes in the terminal of a double cone. **B:** Corresponding pseudocolor images from the double cone plotted in A, with a brightfield DIC image of the isolated double cone. Fluo-4-loaded double cone displayed in B: 1, control, normal (2.5 mM) amphibian superfusate; 2, elevated (50 mM) $[K^+]_o$ containing amphibian superfusate; 3, wash or normal amphibian superfusate; 4, adenosine (50 μM) and elevated $[K^+]_o$ containing superfusate; 5, wash, normal amphibian superfusate; 6, elevated $[K^+]_o$ containing amphibian superfusate; and 7, wash, normal amphibian superfusate. The numbers correspond to time points of image acquisition of A in B. All measurements were made from regions of interest drawn over the terminal and defined as the broad synaptic vesicle-filled extension located under the soma in the perikaryal region (see Materials and Methods). All cells were stimulated with a 1-min application of elevated (50 mM) $[K^+]_o$. **C:** $[Ca^{2+}]_i$ measurements from a large single cone terminal. **D:** $[Ca^{2+}]_i$ measurements from a small single cone terminal. Scale bar = 10 μm.

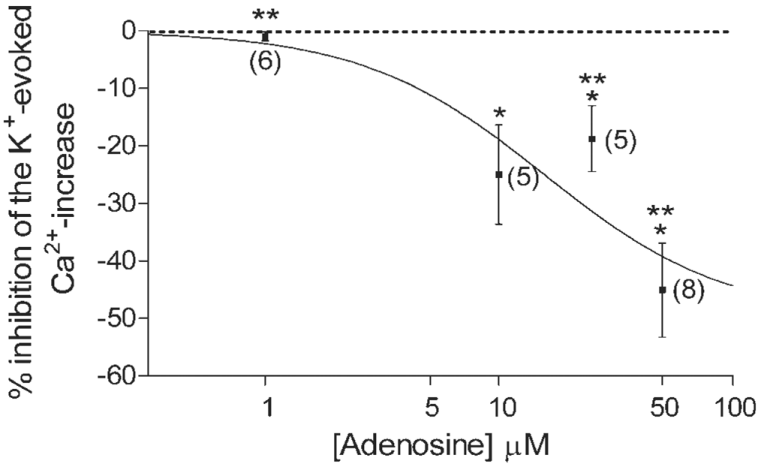

Fig. 6.

Concentration-dependent inhibition of the K^+-evoked $[Ca^{2+}]_i$ increase in isolated cones by adenosine. This graph summarizes the inhibition of the K^+-evoked Ca^{2+} increase in the terminals of all cones tested to different concentrations of adenosine. Fluo-4-loaded cones were stimulated with elevated $[K^+]_o$ in the presence of different concentrations of adenosine (1–50 μM). Inhibition of K^+-evoked change produced by adenosine was normalized to the average of the initial control and the subsequent recovery following the test solution. Each point represents the mean ± SE. Number of experiments is shown in parentheses. ⋆ $P < 0.05$ compared with control. Adenosine concentrations: 1 μM: −1.0% ± 0.8%, n = 6, $P = 0.0908$; 10 μM: −25.0% ± 8.7%, n = 5, $P = 0.0168$, 25 μM: −18.8% ± 5.7%, n = 5, $P = 0.0299$, 50 μM: −45.1% ± 8.2%, n = 8, $P = 0.0009$. ⋆⋆ $P < 0.05$, one-way ANOVA using Neuman-Keuls post hoc multiple-comparisons test shows that the inhibition of the K^+-evoked Ca^{2+} increase by adenosine in cones at 1 μM, 25 μM, and 50 μM are significantly different demonstrating a concentration-dependent effect of adenosine on cones.